Macromolecules

ARTICLE

pubs.acs.org/Macromolecules

A New Technique for Characterizing Comonomer Distribution in Polyolefins: High-Temperature Thermal Gradient Interaction Chromatography (HT-TGIC)

Rongjuan Cong,*,† Willem deGroot,† Al Parrott,† Wallace Yau,† Lonnie Hazlitt,† Ray Brown,† Matt Miller,‡ and Zhe Zhou‡

†Plastics Characterization and ‡Analytical Sciences, The Dow Chemical Company, Freeport, Texas 77541, United States

ABSTRACT: This paper documents a new polyolefin characterization technique, high-temperature thermal gradient interaction chromatography (HT-TGIC or TGIC), to quantify comonomer distribution. A set of homogeneous ethylene−octene homopolymers are used with a commercially available column having a graphitic substrate (HYPERCARB) to demonstrate this technique's applicability to fractionating polyolefins. The separation mechanism appears to be based on the interaction of the polyolefin chains with the graphite surface upon a temperature change in an isocratic solvent. The TGIC technique overcomes the key issues encountered in crystallization based techniques and in high-temperature liquid chromatography with a solvent gradient (HT-LC). Crystallization based techniques cover only a narrow analysis range of 0−9 mol % comonomer content and suffer from potential error in the analysis caused by cocrystallization effects. HT-LC is limited in its capability because of the limited choice in detectors available. Conversely, TGIC, because of the simplicity in solvent composition, has many commercially available detectors, such as infrared detectors (IR), light scattering detectors (LS), and viscometer detectors. For example, a triple detector TGIC with online IR, LS, and viscometer not only is capable of providing comonomer content and distribution from its TGIC retention temperature profile but also can provide a comprehensive microstructure mapping of molecular weight (MW) and intrinsic viscosity (IV) across the comonomer distribution. Under the experimental conditions used in this study, all these features can be obtained in a short analysis time of less than 1 h, for a comonomer content range of from 0 to 50 mol %. Additionally, TGIC is not subject to the cocrystallization problems that traditional polyolefins comonomer distribution characterization techniques have.

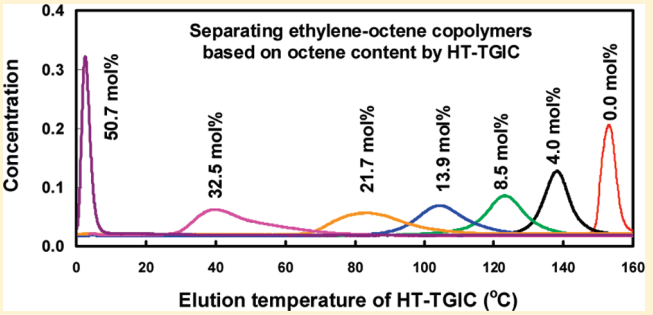

INTRODUCTION

Polyolefins are very important commodity polymers that are part of many products we use in our everyday life. During the past 50 years, polyolefins have become by far the highest volume commercial class of synthetic polymers. With the introduction of new catalysts in the past 20 years, new polyolefin materials with unique structures and properties have been developed.[1−3] Three structural parameters determining material properties include molecular weight (MW) and its distribution (MWD), the comonomer content (CC) and its distribution (CCD), and long chain branching (LCB) and its distribution (LCBD). A complete microstructure characterization is critical to fully control and design physical properties for new polyolefin products. This comprehensive information includes MW and intrinsic viscosity (IV) across CCD and vice versa with CC across MWD and LCBD.

In the past 30 years many analytical techniques have been developed for characterizing the molecular structure of polyolefins. Size exclusion chromatography (SEC)[4] and multiple-detector SEC have been widely used in MW, MWD, and LCB analysis.[5] The techniques for comonomer content and distribution analyses include temperature rising elution fractionation (TREF) with hours of analysis time per sample,[6,7] crystallization analysis fractionation (CRYSTAF) in 3−8 h of analysis per sample,[8,9] and the most recent technique of crystallization elution fractionation (CEF) which gives a fast analysis at about 1 h analysis time per sample.[10] For comprehensive characterization, triple detector (concentration, LS, and viscometer) TREF,[11] triple detector CEF, and two-dimensional techniques such as cross-fractionation[12,13] have been developed to provide a comprehensive microstructure map of MW versus CCD, or comonomer content map versus M_w for polyolefins, in addition to comonomer content and distribution.

Two key challenges associated with crystallization-based CCD analyses of polyolefins, and their related two-dimensional techniques, have been the narrow working range of comonomer

Received: February 10, 2011
Revised: March 4, 2011
Published: March 28, 2011

content and the problematic phenomenon of cocrystallizaiton. All the conventional techniques (including the new CEF technique) are based on the ability of polyolefin chains to crystallize in a dilute solution upon temperature change. Polyolefins with comonomer content up to about 9 mol % are capable of crystallizing in a reasonable time scale. It is possible to extend this limit to ~13 mol % with a prolonged analysis time in dichlorobenzene solvent with subambient temperature capability. Some elastomeric materials with higher comonomer content are unable to crystallize. Cocrystallization has further complicated the separation of multiple-component systems with poor precision and accuracy[14] and made comonomer distribution modeling efforts less fruitful.

To overcome these two key challenges, HT-LC has been developed very recently by using solvent gradient and fully porous spherical graphite particles.[15−18] HT-LC is successfully used to separate polyethylene with octene content from 0 to 100 mol %.[19,20] Crystallization is irrelevant to the separation; thus, cocrystallization is no longer expected to be a concern in HT-LC. The application of HT-LC for polyolefins by using solvent gradients has been recently reviewed by Macko et al.[21]

Unfortunately, HT-LC for polyolefins has its own challenges. First, there is a limitation in the choice of detectors. Generally, polyolefins can only dissolve in a few solvents at an elevated temperature. Solvent choices are further limited by detection to a few preferred chlorinated aromatic solvents. A constantly changing solvent composition prevents one from using typical concentration detectors such as a differential refractive index detector, thus narrowing the choice of usable detectors. One such detector is the evaporative light scattering detector (ELSD). An ELSD detects any nonvolatile component in a sample after nebulization.[22,23] However, ELS detection is known to be nonlinear with respect to concentration as well as solvent composition.[24,25] Another complication is that polyolefin materials often contain nonvolatile additives such as fillers and/or acid neutralizers. This means that ELSD must be calibrated very carefully in order to yield reliable results.[26] All of these factors complicate the use of ELSD in HT-LC for polyolefin comonomer distribution analysis.

The IR-4 detector (Polymer*ChAR*, Spain) has been used for HT-LC with greater success.[19] However, it requires using a specific nonsolvent that minimally absorbs in the wavelength window of the IR-4 detector. This leads to reduced detection sensitivity, a sloped baseline, and the need to adjust HT-LC methods to cover different ranges of comonomer distribution. The second problem, which is probably more severe, is the difficulty in providing comprehensive MW, viscosity, and LCB information across comonomer distribution and vice versa. Constant change in solvent composition, and thus dn/dc, makes the use of online light scattering and viscometer detection difficult. In order to obtain MW information across comonomer distribution, two-dimensional HT-LC hyphenated with SEC (2D HT-LC) has been developed. The 2D HT-LC technique uses a highly efficient SEC column in the second dimension with online LS detector to separate polymer from the nonsolvent peak to allow MW determination of HT-LC fractions.[19] More than 120 fractions from the HT-LC dimension are sent for the second dimension analyses and polymer concentration in each fraction is orders of magnitude lower than the concentration of nonsolvent. In addition to a long analysis time of 9−12 h per sample, the reduced detector sensitivity and increased error from ratioing two weak signals from the online light scattering and concentration detectors are highly undesirable.

Thermal gradient elution chromatography was first reported as a technique for fractionating polymers in 1996 independently by Lochmüller (poly(ethylene glycol))[27] and Chang (polystyrene).[28] This paper describes for the first time the use of TGIC at high temperature or HT-TGIC to quantify comonomer distribution of polyolefins using a commercially available column, HYPERCARB, composed of porous spherical graphite beads as the stationary phase. In HT-TGIC, the separation is achieved by the interaction of polyolefin chains with a graphite surface upon temperature change in an isocratic solvent. This new technique overcomes both the key problems encountered in the crystallization based techniques, i.e., narrow comonomer content analysis range and cocrystallization. It also eliminates the key issues of choice of detectors and inability to provide comprehensive polyolefins structure analysis. Many commercially available detectors can be readily used in HT-TGIC to provide additional information in addition to CCD, such as the MW and IV across comonomer distribution, because of the usage of a single solvent composition. Under the experimental conditions specified in this study, all these features can be obtained in less than 1 h analysis time for a much larger comonomer content range of from 0 to at least 50 mol % than available for crystallization-based techniques.

EXPERIMENTAL SECTION

TGIC Instrumentation. The typical instrument for TGIC can be very similar to a temperature rising elution fractionation (TREF) type of instrument. For our study TGIC was performed with a commercially available crystallization elution fractionation (CEF) instrument (Polymer*ChAR*, Spain) with two-channel IR-4 detector (Polymer*ChAR*, Spain) and a two-angle (15° and 90°) light scattering detector (Precision Detectors, now a part of Agilent) and a two-capillary viscometer. According to the manufacturer of IR-4 detector, the first channel (the measurement channel) corresponds to a broad band collecting all the absorption contributions due to C−H stretching (2800−3000 cm^{-1}); the second channel (the reference channel) is chosen where C−H absorption does not exist. The injection loop was 200 μL unless otherwise stated. Other experimental details are listed in the Results and Discussion.

A Spectra Chrom model CF-1 fraction collector was purchased from Spectrum Chromatography, Houston, TX, and used to collect the fractions from a preparative TGIC fractionation.

Column. A HYPERCARB column, 100 × 4.6 mm i.d. with a particle size of 7 μm and a pore size of 250 Å, was purchased from Thermo Scientific. Zirchrom Diamondbond-C18 column (5 μm, 250 × 4.6 mm i.d., Part DB01-2546) was purchased from Chrom Tech, Inc. Jordi Gel DV8C18 (500A, 150 × 4.6 mm B fittings, Cat. 18500) was purchased from Jordi Associates, F.L.P.

Solvent. *o*-Dichlorobenzene (ODCB, 99% anhydrous grade) and deuterated tetrachloroethane (TCE-d_2) were purchased from Sigma-Aldrich and Cambridge Isotope Laboratories, Inc., respectively. 600 ppm of butylated hydroxytoluene (BHT) was added into ODCB.

Materials. Linear high-density polyethylene standards (HDPE standards) with a peak molecular weight (M_p) ranging from 2155 to 1 100 000 g/mol and polydispersity (M_w/M_n) ranging from 1.01 to 1.21 were purchased from Polymer Laboratories (now a part of Agilent).

Nine randomly polymerized ethylene/α-olefin copolymers (EO-1 to EO-9) were synthesized by using constrained geometry catalyst by The Dow Chemical Co. Detailed information is listed in Table 1. The molecular weight measurement was performed according to ref 29.

Table 1. Characterization Data for EO-1 to EO-9

ethylene octene copolymer	octene (mol %)	MW by conventional GPC (Da)	PDI	catalyst
EO-1	0.0	115 000	2.61	constrained geometry catalyst
EO-2	1.3	104 500	2.08	constrained geometry catalyst
EO-3	4.0	102 900	2.25	constrained geometry catalyst
EO-4	8.5	111 200	2.04	constrained geometry catalyst
EO-5	13.9	123 400	2.01	constrained geometry catalyst
EO-6	19.0	159 839	2.55	constrained geometry catalyst
EO-7	21.7	174 537	2.55	constrained geometry catalyst
EO-8	32.5	235 680	3.26	constrained geometry catalyst
EO-9	50.7	39 595	2.02	constrained geometry catalyst

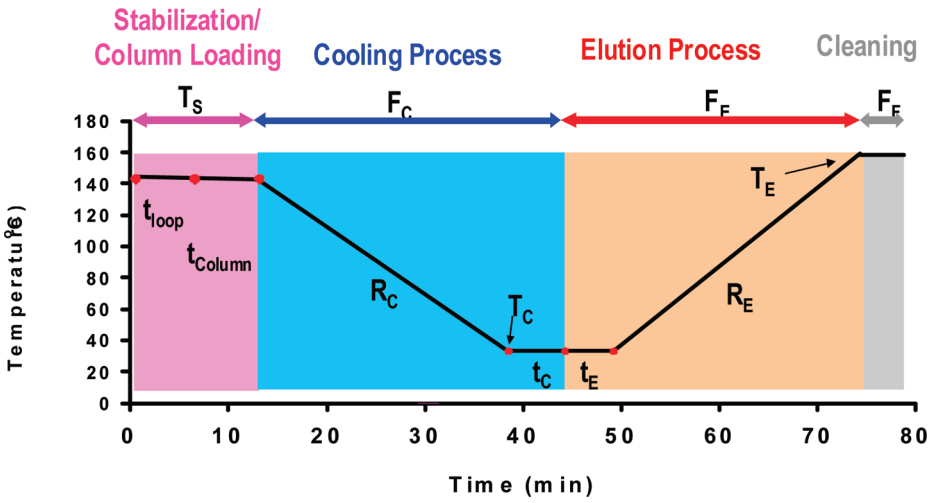

Figure 1. Schematic of HT-TGIC experimental setup. The definitions of each variable are listed in Table 2.

Polymer samples were prepared at 2 mg/mL and dissolved at 160 °C for 2 h by the CEF autosampler unless otherwise stated.

Preparative Fractionation Using Analytical HT-TGIC. Preparative fractionation of HT-TGIC on EO-4 was performed with the instruments specified in the TGIC equipment section. For each injection, nine fractions were collected at 2 min intervals at the beginning of pump initiation for the HT-TGIC elution process. The collection interval and temperature program resulted in each fraction spanning over 6 degrees of the temperature range and occupying 1.4 mL for each fraction. Fractions were collected at eluting temperatures from 90 to 156 °C. Twenty repetitive injections were made, and resulting fractions were combined based upon the temperature range of collection. The resulting polymer solutions were dried with vacuum at 90 °C for about 3 days. ^{13}C NMR analysis was performed on each fraction for octene mol %.

^{13}C NMR Analyses on HT-TGIC Fractions. Each fraction was prepared by adding ~2.7 g of TCE-d_2 with 0.025 M chromium acetylacetonate (relaxation agent) in a 10 mm NMR tube. The sample solution was sparged in a N_2 box for 2 h. The samples were dissolved and homogenized by incubating NMR tubes at 130 °C and vortexing. The ^{13}C NMR spectrum was collected using a Bruker 400 MHz spectrometer equipped with a Bruker Dual DUL high-temperature CryoProbe. The data were acquired using a 7.3 s pulse repetition delay (6 s delay +1.3 s acquisition time), 90° flip angles, and a modified inverse gated decoupling with a sample temperature of 120 °C. All measurements were made on nonspinning samples in locked mode. NMR spectra were analyzed with "linear least-squares analysis with the constraint" reported by Seger et al.[30] to obtain the comonomer content.

RESULTS AND DISCUSSION

HT-TGIC Experimental Setup. The HT-TGIC analysis consists of the following steps: (1) introducing polymer solution into a column at constant temperature; (2) retaining polymer chains onto the column by reducing column temperature; and (3) eluting polymer by raising the column temperature with moderate solvent flow.

The cooling process can be made with or without a slow flow. Without a slow flow during cooling, the analysis is defined as a "static cooling process". With a slow flow during cooling, the analysis is called a "dynamic cooling process". Compared with a static cooling process, the dynamic cooling process may have at least three advantages: (1) reducing the possibility of column plugging due to localized sample concentration build-up by spreading polymer solution along the whole column for practical reasons; (2) further separating retained polymer chains from unretained chains by flushing unretained fractions further down along the column to improve resolution; (3) minimizing the possibility of forming multilayer adsorption effects by retained polymer chains at the same location of the column.

The dynamic cooling process was first proposed by Monrabal et al. during their developing CEF.[10] The benefit of having dynamic crystallization in CEF was to minimize cocrystallization by pushing the uncrystallized fraction downstream in the column. Since HT-TGIC does not involve crystallization, the

Table 2. Definition of the Experimental Variables for TGIC

variable	symbol	description
Stabilization and Sample Loading Process		
stabilization rate (°C/min)	R_S	thermal rate for the temperature changing from the dissolution temperature to the stabilization temperature
stabilization temperature (°C)	T_S	temperature during stabilization and at the start of cooling process
stabilization time (min)	t_{LOOP}	amount of time the sample stays in the injection loop in the top oven of CEF before being loaded into the column
precooling time (min)	t_{COLUMN}	amount of time the sample stays in the front of the column before cooling process begins.
Cooling Process		
cooling rate (°C/min)	R_C	thermal rate of the main oven (where TGIC column is located) during cooling process
final temp of cooling process (°C)	T_C	final temperature at the end of cooling process
postcooling time	t_C	time that the sample stays in the column at the final temperature of cooling process; pump flow rate of cooling process continues but data is not collected
flow rate of pump during cooling process (mL/min)	F_C	flow rate during cooling process; it can be zero (static cooling process) or nonzero (dynamic cooling process)
Elution Process		
elution rate (°C/min)	R_E	thermal rate of the main oven (where TGIC column is located) during elution process
final temperature of elution process (°C)	T_E	final temperature at the end of elution
soluble fraction time	t_E	amount of time that the main oven stays of the final temperature of cooling process while pump being at flow rate of elution process before increasing temperature; data collection begins here; the purpose is to have a well separate SF peak in chromatogram
flow rate of pump during elution process (mL/min)	F_E	flow rate during elution process

dynamic cooling process should improve the resolution over that of a sample fractionated without flow during cooling.

Elution of the polymer can be achieved using a constant heating rate mode, a complex heating rate as a function of time or temperature, or a combination of two modes to further improve resolution. The feasibility of using a complex heating rate depends on the hardware of the instrument.

Experimental Variables of HT-TGIC. TGIC presented in this paper was performed with a commercial crystallization elution fractionation (CEF) instrument (Polymer*ChAR*, Spain) with a constant heating rate elution mode. CEF is a crystallization-based technique. In order to avoid any possible confusion between CEF and HT-TGIC, the nomenclature of HT-TGIC is illustrated in Figure 1. The detailed parameters are listed in Table 2.

The experimental conditions are stabilization temperature (T_s) at 140 °C, stabilization rate (R_s) of 40 °C/min, stabilization time (t_{loop}) of 2 min, and precooling time (t_{column}) of 2 min. Many other factors can affect the results. To simplify the identification of any specific HT-TGIC run conditions, the following run-ID convention is adopted, e.g., TGIC 150 °C_40 °C_180 °C_10 °C/min_2 °C/min_0.035 mL/min_0.5 mL/min represents the following experimental conditions for the TGIC run: stabilization temperature (°C)_final temperature during cooling process (°C)_final temperature during elution process (°C)_cooling rate during cooling process (°C/min)_heating rate during elution process (°C/min)_flow rate during cooling process (mL/min)_flow rate during elution process (mL/min).

Chromatograms of HT-TGIC on Ethylene−Octene Copolymer (EO). The reference materials (EO-1 to EO-9) were made specifically to have narrow comonomer distributions with weight-average molecular weights, M_w, between 35 000 and 236 000 Da by conventional GPC. Figure 2 shows the TGIC chromatograms of EO-1 to EO-9. Except EO-8 with 32.5 mol % octene, all of the EO copolymers show a nearly symmetric peak shape. The elution temperature of the nine EO copolymers is in the order of EO-1 > EO-2 > EO-3 > EO-4 > EO-5 > EO-6 > EO-7 > EO-8 > EO-9, where EO-9 with octene content of 50.7 mol % was not retained under the current TGIC experimental conditions (see Figure 2 caption for run ID). EO-9 appeared at 2.6 °C instead of eluting at 0 °C. This is due to the presence of a small volume that polymer solution has to travel before reaching the concentration detector. This small volume is commonly referred to as the delay volume. Delay volume can be converted into temperature by multiplying by heating rate during the elution process and then being divided by the flow rate during elution process. The peak temperature of the TGIC chromatogram is defined as the temperature at the highest peak height minus the delay volume (in terms of temperature, °C). The peak temperature of the nine EO copolymers is plotted against octene mol % (Figure 3). Peak temperature decreases with octene mol %. This is the first time that it has been demonstrated that HT-TGIC can be used to determine the comonomer distribution and content of polyolefin copolymers.

In general, homogeneously prepared EO polymers with octene content higher than 10 mol % are mostly amorphous materials. These polymers are unretained when analyzed using crystallization-based characterization techniques such as TREF, CEF, or CRYSTAF. However, EO-5, EO-6, EO-7, and EO-8 which contain higher than 13.0 mol % octene are all retained in the TGIC column as is seen in Figure 2. The peak temperature of HDPE with zero octene content (EO-1) is 150.4 °C. This elution temperature is about 49 °C higher than the peak elution temperature in TREF and CEF and ~15 °C higher than the melting peak temperature of DSC. This clearly demonstrates the strong attraction that the graphite has for polyethylene.

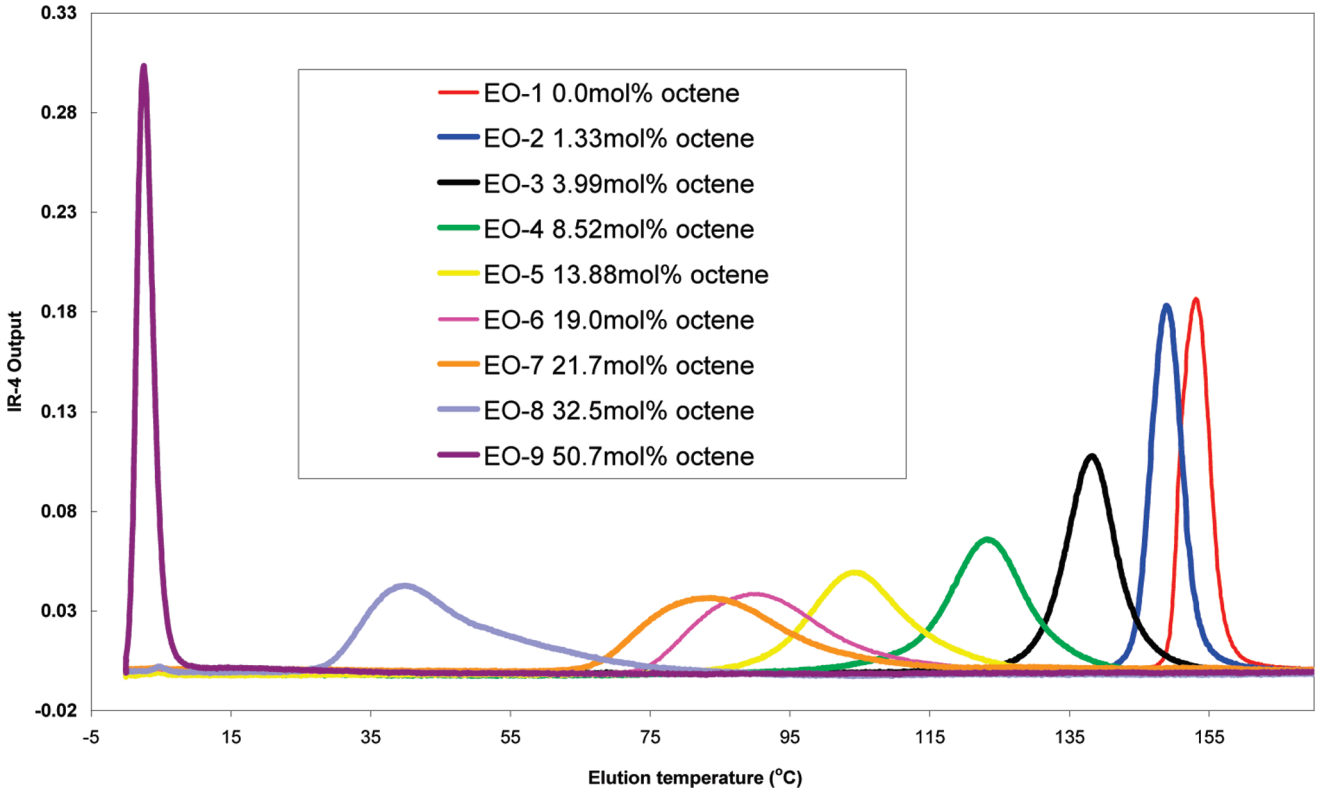

Figure 2. TGIC chromatograms of EO-1 to EO-9. HYPERCARB column (100 × 4.6 mm, 7 μm particle size). The TGIC experimental conditions (stabilization temperature_final temperature during cooling process_final temperature during elution process_cooling rate during cooling process_heating rate during elution processs_flow rate during cooling process_flow rate during elution process) are 140 °C_0 °C_175 °C_ 6 °C/min_3 °C/min_0.03 mL/min_0.5 mL/min.

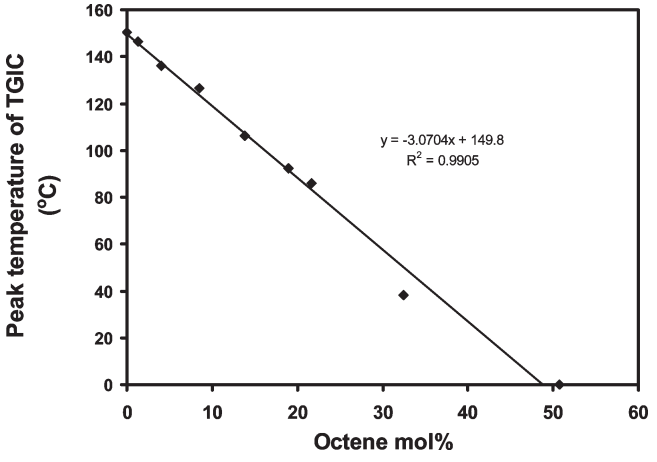

Figure 3. Plot of the peak temperature of TGIC chromatograms of EO-1 to EO-9 versus octene mol %. HYPERCARB column (100 × 4.6 mm, 7 μm particle size). The TGIC experimental conditions are 140 °C_0 °C_175 °C_6 °C/min_3 °C/min_0.03 mL/min_0.5 mL/min.

n-Alkanes (C16−C32) were reported to have adsorptive interactions with graphitized carbon as early as in 1987.[31] These results suggest the possible adsorptive interactions between polyolefin chains with graphite of HYPERCARB column leading to HT-TGIC separation, not crystallization. Furthermore, it shows that this interaction is a function of comonomer content. It is clear from Figure 2 that HT-TGIC is capable of analyzing a wider range comonomer content of 0−50 mol % than any of the conventional crystallization based techniques, which is typically 0−9 mol % octene. A further study of the interaction is underway to help with future efforts to optimize HT-TGIC experimental conditions.

^{13}C NMR Results of Each Fraction from Preparative HT-TGIC. To further study the separation mechanism of HT-TGIC for polyolefins, EO-4 sample (MW 112 000 Da) was chosen for preparative HT-TGIC fractionation, as described in the Experimental Section. Each fraction from preparative HT-TGIC fractionation was recovered and analyzed by ^{13}C NMR for comonomer content with the method.[32−34] The TGIC chromatogram of EO-4 is shown in Figure 4. The peak centered around 96 °C represents the amount of the material that is soluble (not retained by the column) at 90 °C. This portion of material would have been retained by the column if the final temperature of cooling processing was set at 0 °C as the TGIC method used in Figure 2. The temperature range of each fraction collected by preparative HT-TGIC is also shown in Figure 4. Figure 5 shows the ^{13}C NMR spectrum for fraction 5 and shows a typical ethylene−octene spectrum at an estimated concentration of 3.2 mg/mL. A small amount of impurity shown at 30.9 ppm and 25.0 ppm were from unknown sources. Octene mol % of the fractions versus the temperature cut for each fraction is plotted in Figure 6. Octene mol % is shown to decrease with increasing temperature. These results unambiguously prove that HT-TGIC separates randomly polymerized EO according to octene content.

In general, preparative fractionation is performed with a preparative column having a larger diameter and higher flow

dx.doi.org/10.1021/ma200304e |*Macromolecules* 2011, 44, 3062–3072

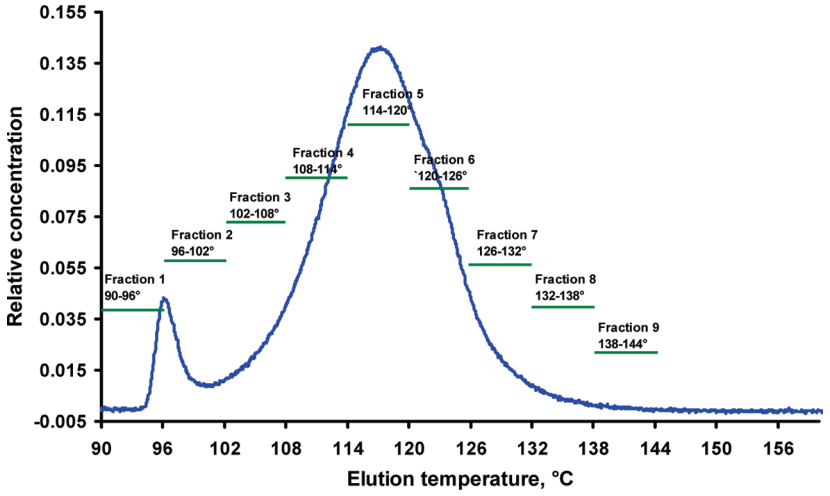

Figure 4. TGIC chromatogram of EO-4 copolymer. The temperature cut for each fraction is labeled. The TGIC experimental conditions are 110 °C_ 90 °C_170 °C_10 °C/min_3 °C/min_0 mL/min_0.7 mL/min. Sample concentration was at 4 mg/mL.

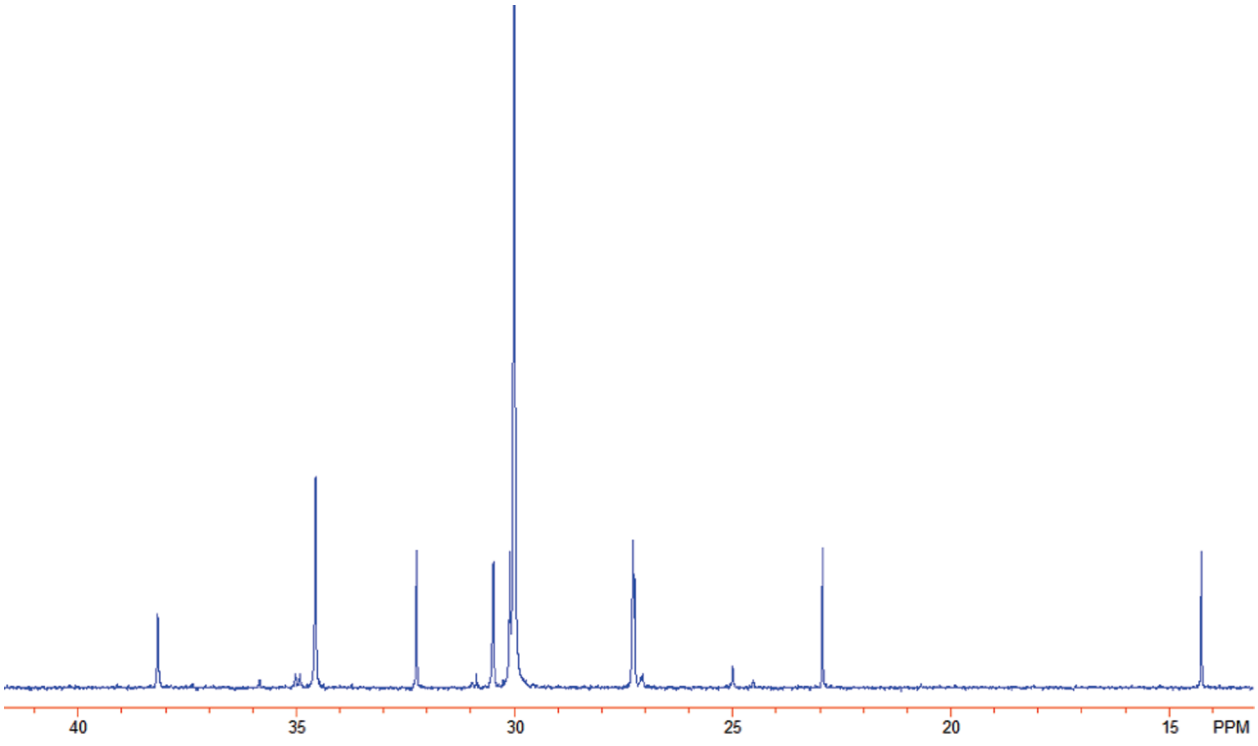

Figure 5. ^{13}C NMR of the fraction 5 (114−120 °C) of EO-4. The sample concentration was 3.2 mg/mL. Peak assignment was made according to ref 32.

rates than commonly employed with an analytical column. However, the preparative fractionation in this study was performed with the same analytical TGIC instrument used in Figures 2 and 3. The dramatic improvement in signal-to-noise with a cryoprobe for high-temperature polyolefin NMR[35,36] provides us this great opportunity to perform ^{13}C NMR on a limited quantity of materials with a reasonable acquisition time for a sample concentration as low as 0.9 mg/mL to 3.2 mg/mL. These concentrations are a few hundredths of the concentration usually used in ^{13}C NMR analysis with conventional probe. The method reported here had led to a change in the concept of preparative fractionation. Preparative fractionation can be performed on an analytical scale instrument with a limited number of repeat injections. This new approach dramatically reduces solvent usage, the time, and the effort to set up a preparative instrument with a preparative column and simplifies sample recovery.

A legitimate question is "how much of role does molecular weight play in the TGIC fractionation mechanism?" Very limited materials but sufficient for ^{13}C NMR analysis with a high-temperature cryoprobe were collected for each fraction in this preparative study. Recovering the materials after NMR analysis for further GPC analysis was not feasible due to the existence of chromium acetylacetonate (relaxation agent)

being added during NMR analysis. However, one of the key reasons to choose EO-4 in this preparative study was because of its MW of 111 200 and polydispersity of 2.04. This may minimize the effect of MW. A more detailed study of the MW effect is given in a later section by using narrow polydispersity standards.

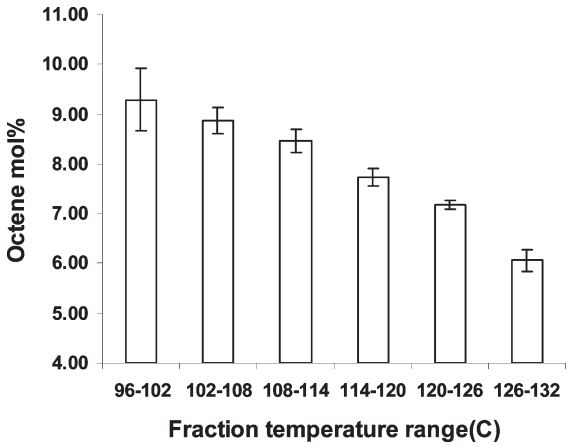

Figure 6. Octene content of different fractions collected from preparative fractionation of EO-4. The TGIC experimental conditions are 110 °C_ 90 °C_170 °C_10 °C/min_3 °C/min_0 mL/min_0.7 mL/min.

Anchoring Temperature and Desorption Temperature of HDPE on HYPERCARB Column. To further understand the TGIC separation mechanism, a specific experiment was designed by setting TGIC experiments with stabilization temperature being equal to the final temperature of cooling process and with a static cooling process (no flow during the cooling process). The purpose is to determine the temperatures at which polyolefin chains start to be retained by the HYPERCARB column and start to be eluted from the column. EO-1 was chosen for this study because of its simplicity in microstructure with zero octene content. Figure 7A shows HT-TGIC chromatograms of EO-1 obtained when the stabilization temperature is equal to the final temperature of cooling process (120, 130, 135, and 140 °C, respectively).

When stabilization temperature and final temperature during the cooling process are at 140 °C, there is no significant retention of EO-1 by the HYPERCARB column; i.e., the chains prefer to

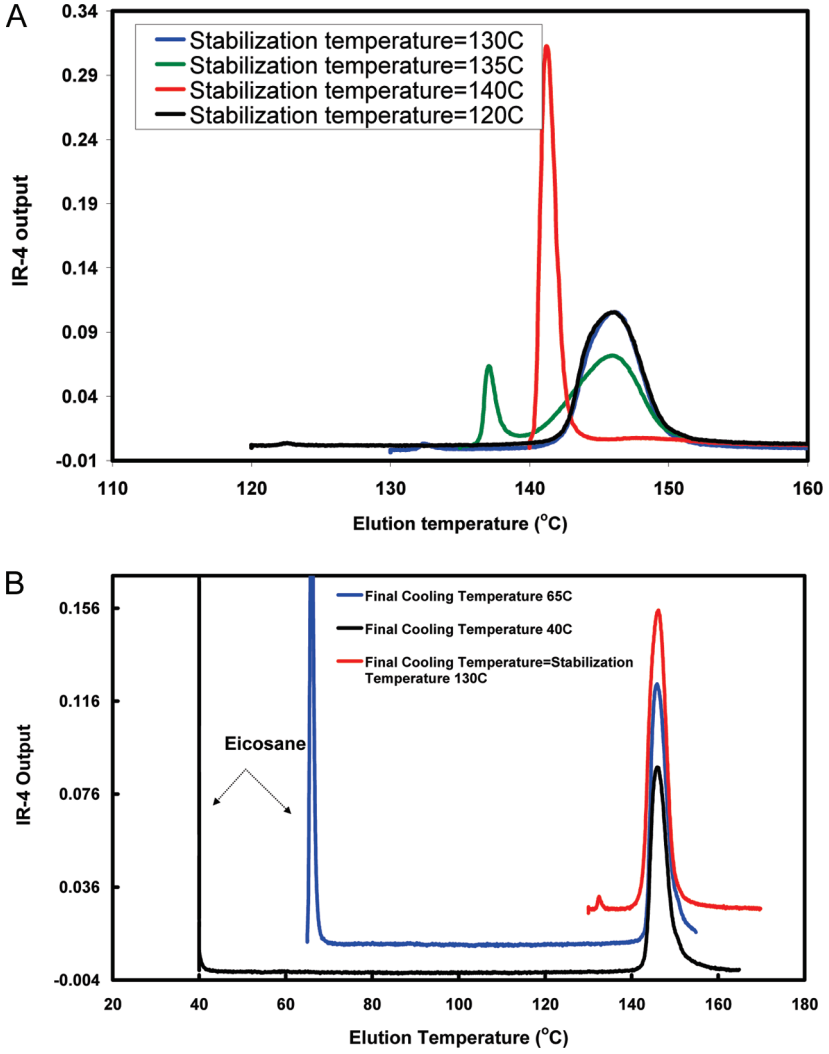

Figure 7. (A) TGIC chromatograms of EO-1from IR-4 detectors with HYPERCARB column. The TGIC experimental conditions are stabilization temperature (°C)_final temperature during cooling process (°C)_175 °C_0 °C/min_2 °C/min_0 mL/min_0.7 mL/min. (B) TGIC chromatograms of EO-1 from IR-4 detectors with HYPERCARB column.

dx.doi.org/10.1021/ma200304e |*Macromolecules* 2011, 44, 3062–3072

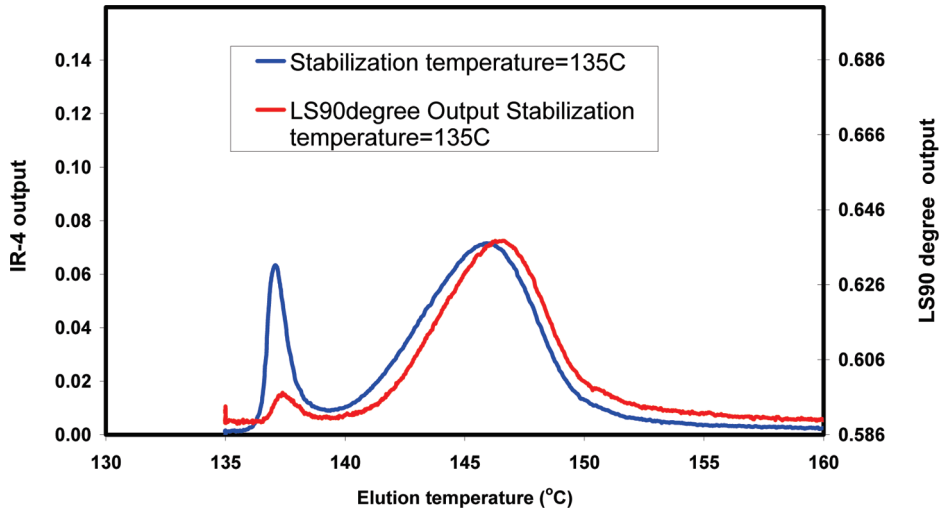

Figure 8. TGIC chromatograms of EO-1 from IR-4 detector and online LS detector at 90° angle. The TGIC experimental conditions are 135 °C_135 °C_175 °C_0 °C/min_2 °C/min_0 mL/min_0.7 mL/min.

remain in solution. EO-1 elutes essentially at the same temperature as stabilization temperature after subtracting the effect of the delay volume on elution temperature. The chromatogram is a sharp peak with a width at half peak height being <1.7 °C. This is a normal degree of chromatographic band broadening expected under the experimental conditions by using a 200 μL injection loop size. When stabilization temperature and final temperature during the cooling process are 135 °C, a majority of EO-1 is retained by the HYPERCARB column (with a small unretained peak at lower temperature, to be discussed later). It appears as a broad peak eluting at a temperature higher than 140 °C. When stabilization temperature and final temperature during the cooling process are 130 °C, almost all of the EO-1 is retained. It appears as a broad peak at temperature higher than 140 °C. The onset of HT-TGIC retention (or anchoring) temperature for EO-1 is seen here to be between 130 and 135 °C, while the normal crystallization temperature of HDPE (EO-1) in ODCB at similar concentration is measured at ~85 °C by CRYSTAF. The retention temperature of EO-1 in TGIC is ~50 °C higher than the crystallization temperature in ODCB. This result supports the existence of high adsorption energy between EO-1 and graphite. A further lowering of the stabilization temperature and final temperature during the cooling process to 120 °C results in no change in the chromatogram. As a matter of fact, the elution chromatograms of TGIC for HDPE at the stabilization temperature being 130 and 120 °C overlay very well, as shown in Figure 7A.

Figure 7B shows the TGIC chromatograms of EO-1 obtained by using the methods cooling down to 130, 65, and 40 °C. For the experiments performed at final cooling temperature at 65 and 40 °C, a certain amount of eicosane was added into EO-1. When final cooling temperature is set at 65 and 40 °C, eicosane is not retained by the HYPERCARB column and thus appears as a sharp peak at the temperature of 65 and 40 °C. On the other hand, the retained HDPE (EO-1) shows as a broad peak at elution temperature of 146 °C.

When stabilization temperature and final temperature during the cooling process are 135 °C, there is a small unretained fraction which appears as a unique peak mode at 137 °C in Figure 7. To understand this feature, the chromatograms from online light scattering signal and IR-4 detector are plotted in Figure 8. LS detector had a much smaller peak than the IR-4 concentration detector for the sharp peak. LS detector shows a similar peak size as the concentration detector for the broad main peak. This information indicates that the small sharp peak at low temperature originated from a low molecular weight fraction of EO-1. This result suggests that there is some molecular weight effect in TGIC. The detailed discussion about the extent of the MW effect will be given in later section.

Another point to discuss is the peak broadness in Figure 7. HDPE (EO-1) is retained onto the HYPERCARB column at a narrow temperature range between 130 and 135 °C under the experimental conditions specified here. The unretained EO-1 peak resulting from the run as stabilization temperature and final cooling temperature during cooling process at 140 °C elutes at a peak temperature of 142 °C (without deducting the delay volume). The peak width at the half height is about 1.7 °C. On the other hand, retained EO-1 elutes at a peak temperature of 147 °C (without deducting the delay volume) with a peak width at the half height of about 5 °C. The elution peak spans a much large temperature range from about 140 to 155 °C. There is an ~200% increase in peak width. This increased in band broadening should be mainly due to the interaction of EO-1 with column because it happens only to retained polymer.

Various factors may have played important roles in this extra band broadening due to this interactive process. One factor might be the pore size of the HYPERCARB column packing (250 Å) being too small for some large chains. However, in a separate study, we found that a similar degree of band broadening is observed with narrow distributed HDPE samples and also with hexacontane and tetratetracontane samples. Hexacontane and tetratetracontane are compounds with a single chemical structure and monodispersed in MW by definition. They both have chain length with MW less than 1000 and should not be excluded from 250 Å pore in the HYPERCARB column packing. These results suggest that the observed broadness in the HT-TGIC retained peak might not be caused directly by the pore sizes being too small in the HYPERCARB column. The other factor is the possible surface inhomogeneity of HYPERCARB column. Chain

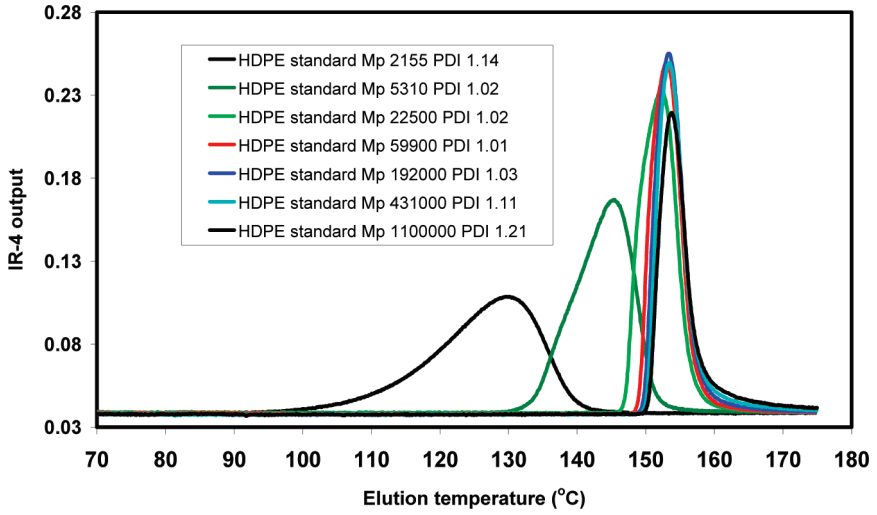

Figure 9. TGIC chromatograms of HDPE standards with M_p from 2155 to 1 100 000. The TGIC experimental conditions are 140 °C_40 °C_175 °C_6 °C/min_3 °C/min_0.03 mL/min_0.5 mL/min.

retention happens once one unit of polymer chain is adsorbed onto the substrate. Because of the flexibility of the chain, various changes in chain conformation may happen after initial chain retention. This leads to the thermodynamically most favorable conformation with multiple chain segments being adsorbed onto the substrate. This conformation optimization process may lead to a further difference in the strength of the interaction between retained chain and substrate because the substrate may have local variations in surface properties. The extra band broadening may be also related to the highly porous structure of graphite of the HYPERCARB column. Some detached polymer chains may travel tortuous paths before leaving the column. Various attempts have been made to reduce extra band broadening without much success through the modification of experimental conditions such as cooling and heating rates with HYPERCARB column with 100 × 4.6 mm and 250 Å pore size. On the basis of our understanding about the HT-TGIC separation mechanism, a large surface area but not highly porous structure is needed to provide sufficient sites for interaction. Limiting the highly porous structure of graphite may be one option to minimize this extra band broadening.

Another point to discuss is a much narrower temperature range observed during the anchoring process compared to the elution process. This may suggest that a high resolution may be achieved by only using the cooling process for analysis instead of the heating process. Of course, a significant effort is needed to modify hardware in order to produce results using only the cooling process of TGIC analysis.

Other columns were evaluated to further understand if the interaction between graphite with polyolefins is a critical factor in HT-TGIC techniques. The other analytical columns tested in TGIC experiments were Zirchrom Diamondbond-C18 column (5 μm, 250 × 4.6 mm i.d., Part DB01-2546), and Jordi Gel DVBC18 (500A, 150 × 4.6 mm B fittings, Cat. 18500). No effective HT-TGIC was obtained, and the separation results were similar to CEF. These results reinforce the importance of the flat sheet structure of graphite.

Various literature reports have predicted that elution during a thermal gradient is related to the choice of solvent.[26] Trichlorobenzene was tried as the solvent for TGIC. The anchoring

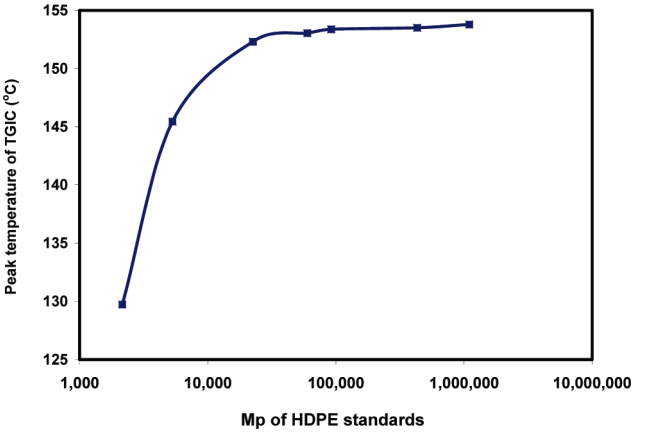

Figure 10. Peak temperature of TGIC chromatograms of HDPE standards versus molecular weight. The TGIC experimental conditions are 140 °C_40 °C_175 °C_6 °C/min_3 °C/min_0.03 mL/min_0.5 mL/min.

temperature of EO-1 in TCB is in a narrow temperature of 120−125 °C, while the elution happens approximately at 145 °C with an even larger temperature range (broader than in ODCB). TCB and ODCB are widely accepted as good solvents for polyolefins. No significant difference in crystallization based techniques has been reported between TCB and ODCB in the literature. Similarly, numerous experiments conducted by the authors have not demonstrated any differences between these two solvents when crystallization-based techniques are used. The differences observed in TGIC between using ODCB and TCB may support that solvent strength is likely to be another important factor affecting retention in HT-TGIC for polyolefins. Work is underway by purposefully doping a certain amount of nonsolvent into a good solvent to form an isocratic solvent.

Investigation of Molecular Weight Effect in TGIC. The earlier result in Figure 8 indicates that there is some degree of M_w effect in TGIC. MW dependence in interaction chromatography has been widely proposed as a general factor for polymer chromatography.[37] A recent model predicts polymer elution to increase with, decrease with, or be independent of MW

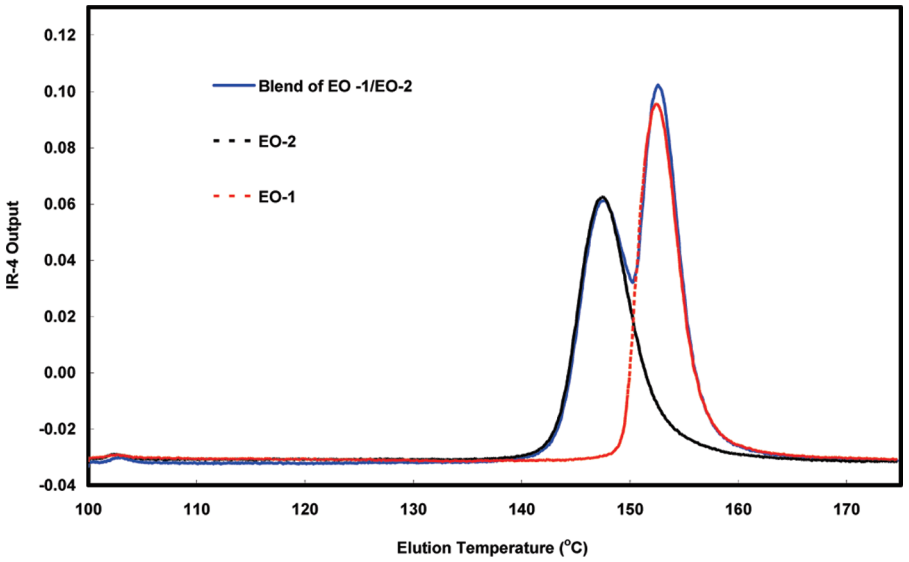

Figure 11. TGIC chromatograms of a blend of EO-1/EO-2 at 50:50 (w:w), EO-1, and EO-2. The TGIC experimental conditions are 140 °C_ 100 °C_175 °C_6 °C/min_3 °C/min_0.10 mL/min_0.5 mL/min.

depending on the balance of chromatographic interactions.[38] To quantify the effect of MW, HDPE standards (Polymer Laboratories, a part of Agilent) with different MW and molecular weight distribution are investigated. Figure 9 shows the chromatograms of HDPE standards with M_p (the peak MW) ranging from 2155 to 1 100 000 Da and polydispersities ranging from 1.01 to 1.21. Peak temperature of each HDPE is plotted against M_p, as shown in Figure 10. Peak temperature increased with M_w initially and reached a plateau at M_p of 22 500 Da. This level of MW effects also was seen in crystallization-based techniques.[39] In this specific application, TGIC is intended to analyze the comonomer distribution of polyolefins. Only polyolefins with significant MW (generally over 25 000 Da to a couple of million of daltons) are generally of interest for commercial applications. An online LS detector provides the unique advantage of being capable of distinguishing the sources of HT-TGIC retention, whether it is due to low MW or high comonomer content. A similar investigation is needed for polyolefins with high comonomer content in the future to get a better overall understanding about M_w effect in TGIC for polyolefin.

Minimization of Cocrystallization. When discussing comonomer distribution analysis, cocrystallization refers to the phenomena that chains with similar microstructure form crystals together. Cocrystallization is one of the key factors limiting the resolution of crystallization-based techniques. It is very challenging to quantify the degree of cocrystallization. Because of this problem of cocrystallization, modeling or deconvolution of CRYSTAF, TREF, and CEF chromatograms for multiple component systems has been found to be very difficult. TGIC does not separate EO polymers based on crystallization. The retention temperature in HT-TGIC is well above the crystallization temperature usually observed in crystallization-based techniques. Therefore, it is expected that cocrystallization will not take place in the HT-TGIC experiment, which can be one of the most important advantages of TGIC over TREF, CEF, CRYSTAF, and DSC.

To support this concept, a blend of EO-1 and EO-2 was made by solution blending at 50:50 (w:w) of EO1 and EO-2. The blend was analyzed together with EO-1 and EO-2. The TGIC method was purposefully chosen such that the final temperature of cooling process was set as 100 °C. It is well-known that HDPE does not crystallize out from a dilute solution at 100 °C. Figure 11 shows the TGIC chromatograms of EO-1, EO-2, and the blend of EO-1/EO-2 at 50:50 (w:w). The chromatogram of the blend overlays very well with EO-1 at high temperature and with EO-2 at low temperature. No shift in the peak temperatures was observed between the blend and individual components. This result supports the absence of the cocrystallization which is often observed in crystallization-based techniques.

CONCLUSIONS

This is the first time that TGIC has been successfully used in quantifying comonomer content and distribution for polyolefins. The key characteristics of HT-TGIC include the following:

(1) The interaction of polyolefins chains with graphite substrate seems to be the key to HT-TGIC.

(2) HT-TGIC separation provides a much larger range of comonomer content than all the crystallization-based techniques.

(3) TGIC retention temperatures are all well above the crystallization temperature usually observed for polyolefin chains. Therefore, cocrystallization may no longer be a concern.

(4) With constant solvent composition, HT-TGIC can be equipped with multiple detectors including LS and viscometer detector to provide a comprehensive microstructure characterization for polyolefins.

(5) There is a weak MW dependence in HT-TGIC at a comparable level seen in crystallization-based techniques. The ability of HT-TGIC to use a LS detector is helpful to study and account for this MW dependence.

(6) The observation of large differences in HT-TGIC between ODCB and TCB suggests another important factor to be controlled in HT-TGIC experiment by varying solvent strength. It can be done by the addition of poor solvent and run the solvent mixture in an isocratic TGIC mode. This may lead to an even wider separation window for comonomer content from current 0−50 to 0−100 mol % and possibly increase the resolution for the samples with very low comonomer content.

(7) There is substantial band broadening caused by some factors not well understood at this moment. An in-depth investigation is needed in order to improve TGIC resolution capability.

AUTHOR INFORMATION

Corresponding Author
*E-mail: rcong@dow.com.

REFERENCES

(1) McKnight, A. L.; Waymouth, R. M. *Chem. Rev.* **1998**, *98*, 2587–2598.
(2) Lai, S. Y.; Wilson, J. R.; Knight, G. W.; Stevens, J. C. US Patent 5,272,236, 1993.
(3) Arriola, D. J.; Carnahan, P. D.; Hustad, P. D.; Kuhlman, R. L.; Wenzel, T. T. *Science* **2006**, *312*, 714–719.
(4) Yau, W. W.; Kirkland, J. J.; Bly, D. D. *Modern Size-Exclusion Liquid Chromatography*; John Wiley and Sons, Inc.: New York, 1979.
(5) Wood-Adams, P. M.; Dealy, J. M.; deGroot, A. W.; Redwine, O. D. *Macromolecules* **2000**, *33*, 7489–7499.
(6) Wild, L. *Adv. Polym. Sci.* **1990**, *98*, 1–47.
(7) Hazlitt, L. G. *J. Appl. Polym. Sci., Appl. Polym. Symp.* **1990**, *45*, 25–37.
(8) Monrabal, B. *J. Appl. Polym. Sci.* **1994**, *52*, 491–499.
(9) Soares, J. B. P. *Macromol Theory Simul.* **1995**, *4*, 305–324.
(10) Monrabal, B.; Sancho-Tello, J.; Mayo, N.; Romero, L. *Macromol. Symp.* **2007**, *257*, 71–79.
(11) Gillespie, D. T.; Yau, W. W. *TAPPI Polym., Laminations, Coat. Conf., Proc.* **2000**, *2*, 699–707.
(12) Nakano, S.; Goto, Y. *J. Polym. Sci.* **1981**, *26*, 4217–4231.
(13) Gillespie, D. T.; Li Pi Shan, C.; Hazlitt, L. G.; deGroot, A. W.; Arnoudse, P. B.; Williams, C. A. WO 2006/081116 A1, 2006.
(14) Hermel, T.; Cong, R. *Polym. Prepr.* **2010**, *51*, 95–96.
(15) Macko, T.; Brüll, R.; Alamo, R. G.; Thomann, T.; Grumel, V. *Polymer* **2009**, *50*, 5443–5448.
(16) Pasch, H.; Albrecht, A.; Brüll, R.; Macko, T.; Hiller, W. *Macromol. Symp.* **2009**, *282*, 71–80.
(17) Tibor, M.; Pasch, H. *Macromolecules* **2009**, *42*, 6063–6067.
(18) Miller, M. D.; deGroot, A. W.; Lyons, J. L.; Winniford, W. L.; Van Damme, F. A. Patent application PCT/US2009/059261, 2009.
(19) Roy, A.; Miller, M. D.; Meunier, D. M.; de Groot, A. W.; Winniford, W L.; Van Damme, F. A.; Pell, R. J.; Lyons, J. W. *Macromolecules* **2010**, *43*, 3710–3720.
(20) Miller, M. D.; deGroot, A. W.; Lyons, J. L.; Winniford, W. L.; Van Damme, F. A. *J. Polym. Sci.*, accepted for publication.
(21) Macko, T.; Brüll, R.; Zhu, Y.; Wang, Y. *J. Sep. Sci.* **2010**, *33*, 3446–3454.
(22) Chen, S. S. *Encycl. Chromatogr. (3rd Ed.)* **2010**, *1*, 818–820.
(23) Trathnigg, B.; Kollroser, M. *J. Chromatogr. A* **1997**, *768*, 223–238.
(24) Mathews, B. T.; Higginson, P. D.; Lyons, R.; Mitchell, J. C.; Sach, N. W.; Snowden, M. J.; Taylor, M. R.; Wright, A. G. *Chromatographia* **2004**, *60*, 625–633.
(25) Kohler, M.; Haerdi, W.; Christen, P.; Veuthey, J. L. *Trends Anal. Chem.* **1997**, *16*, 475–484.
(26) Pasch, H.; Trathnigg, B. *HPLC of Polymers*; Springer-Verlag: Berlin, 1999; p 35.
(27) Lochmüller, C. H.; Moebus, M. A.; Liu, Q. C.; Jiang, C.; Elomaa, M. *J. Chromatogr. Sci.* **1996**, *34*, 69–76.
(28) Lee, H. C.; Chang, T. *Polymer* **1996**, *37*, 5747–5749.
(29) Karjala, T. P.; Sammler, R. L.; Mangnus, M. A.; Hazlitt, L.; Johnson, M. S.; Hagen, C. M.; Huang, J. W. L.; Reichek, K. N. *Annu. Tech. Conf. - Soc. Plast. Eng.* **2008**, *66*, 887–891.
(30) Seger, M. R.; Maceil, G. E. *Anal. Chem.* **2004**, *76*, 5734–5747.
(31) Findenegg, G. H.; Liphand, M. *Carbon* **1987**, *25*, 119–128.
(32) Randall, J. C. *Rev. Macromol. Chem. Phys.* **1989**, *C29*, 201–317.
(33) Qiu, X.; Zhou, Z.; Gobbi, G.; Redwine, D. *Anal. Chem.* **2009**, *81*, 8585–8589.
(34) Seger, M. R.; Maciel, G. E. *Anal. Chem.* **2004**, *76*, 5734–5747.
(35) Zhou, Z.; Kuemmerle, R.; Stevens, J. C.; Redwine, D.; He, Y.; Qiu, X.; Cong, R.; Klosin, J.; Montanez, N.; Roof, G. *J. Magn. Reson.* **2009**, *200*, 328–333.
(36) Zhou, Z.; Stevens, J. C.; Klosin, J.; Kummerle, R.; Qiu, X.; Redwine, D.; Cong, R.; Taha, A.; Mason, J.; Winniford, B.; Chauvel, P.; Montanez, N. *Macromolecules* **2009**, *42*, 2291–2292.
(37) Pasch, H.; Trathnigg, B. *HPLC of Polymers*; Springer-Verlag: Berlin, 1999; pp 17−22.
(38) Radke, W.; Lee, S.; Chang, T. Y. *J. Sep. Sci.* **2010**, *33*, 3578–3583.
(39) Nieto, J.; Oswald, T.; Blanco, F.; Soares, J. B. P.; Monrabal, B. *J. Polym. Sci., Part B: Polym. Phys.* **2001**, *39*, 616–1628.